# Minimizing the Perception of Chromatic Noise in Digital Images

*Xiaoyan Song, Garrett M. Johnson and Mark D. Fairchild*
*Munsell Color Science Laboratory*
*Rochester Institute of Technology, Rochester, New York, USA*

## Abstract

A psychophysical experiment was performed to measure the visibility of chromatic noise. Through Principle Component Analysis (PCA) on the results of this experiment, an orthogonal color space with the luminance channel independent of chromatic channels was constructed. By transforming noise images into this space, the visibility of chromatic noise can be predicted. Comparison with other opponent color spaces illustrates their relative properties regarding cross-talk of chromatic noise into the luminance channel (or vice versa).

## 1. Introduction

In digital imaging, the problem of reducing the amount of data required to represent a digital image is addressed by image compression. Redundant data are removed for reducing the storage required to save an image or the bandwidth required to transmit it. Transformation from a 2-D pixel array into a statistically uncorrelated data set is applied prior to storage or transmission of the image.[1] In digital photography, there is a need to minimize noise or artifacts in the luminance channel and put it into the less perceptible chrominance channels. For image quality and image difference metrics, images are first transformed into an opponent color space for efficient computation and spatial processing such as spatial filtering or chromatic subsampling.[2,3] Ideally the opponent color space would be orthogonal so that any processing performed on one channel does not affect the other channels.

Opponent color encoding, as described by Hering, is an important concept in color appearance. The existence of opponent colors provides an efficient neural representation of color by decorrelating the cone absorptions that represent an inefficiency in the visual coding of spectral information.[4] The idea of efficient transmission of opponent coding was also supported by Buchsbaum and Gottschalk from the point of view of information theory.[5] Psychophysical experiments have shown that the human visual mechanisms can be separable in pattern and color.[6,7] There are three cone types in the retina that are sensitive to short (S), middle (M) and long (L) wavelengths of visible light. The three signals are then transformed to opponent signals by the neurons of the retina before being passed on to the brain. The summation of the three cone types (L+M+S) produces an achromatic response. Differentials of the cone signals constitute chromatic opponent signals: red-green (L-M+S) and yellow-blue (L+M-S).

Contrast sensitivity functions describe the visual system's sensitivity to harmonic stimuli as a function of spatial or temporal frequency. They change with spatial frequency and background mean luminance. Research has shown that the achromatic, or luminance, contrast sensitivity function peaks at an intermediate spatial frequency, and the low or high frequency sensitivity diminishes.[4] Weber's Law indicates that the threshold increases roughly in proportion to mean background intensity. It is universally accepted that the luminance mechanism has the highest spatial resolution and that the contrast sensitivity functions (CSFs) are band-pass for luminance channel, and low-pass for the chromatic channels.[7,8] Owen et al. did measurements of CSFs in not only red-green and yellow-blue directions but also in lime-purple and cyan-orange directions, resulting in low-pass consistency for all chromatic directions.[9] Since contrast sensitivity functions describe the opponent response to complex stimuli, describing an image in an opponent color space makes sense for application of the contrast sensitivity functions as spatial filters. There are many opponent color spaces described in literature. Different color spaces have been designed for specific applications. Below, the YCbCr, YIQ and IPT space are described briefly as examples.

YCbCr space is a subset of YUV that scales and shifts the chrominance values into the range of 0 and 1. It is often used in component digital video such as studio video, JPEG, and MPEG.[10]

YIQ space is a television broadcast standard first adopted by the National Television Standards Committee (NTSC) of the United States for broadcast television in 1953. The purpose of using YIQ space in television broadcast was to"maximize the perceptual resolution of the encoded color information using the fixed amount of bandwidth available in a broadcast signal in such a way as to be compatible with black and white transmission."[11] The *Y* channel is used for encoding luminance information, the *I* axis encodes chrominance along a blue-green to orange vector, and *Q* along a yellow-green to magenta vector.

IPT color space has been developed to be more uniform in perceived hue than traditional color spaces such as CIELAB.[12] This attribute leads it very useful in image processing application such as gamut mapping. The lightness dimension is denoted as *I*, the red-green dimension is *P*, and the yellow-blue dimension is *T*. The input of the model is CIEXYZ for the 1931 2-degree observer with an illuminant of D65. It includes two linear transforms and an exponent transform. IPT space has been tested by Zhu et al. and showed good performance in space uniformity and hue constancy.[13]

Borer and Süsstrunk[14] introduced an opponent color space with three components of blue-yellow, red-green, and green-red, aiming to mimic the color processing in the primate retina. Spatial extension was used to distinguish the last two.

In the present paper, a psychophysical experiment was performed using the method of adjustment for subjects to adjust chromatic noise image until it is least perceptible. A preliminary orthogonal space was derived by performing PCA on the experimental data. Principal Components Analysis (PCA) is a powerful technique to generate a set of principal components orthogonal dimensions, avoiding redundant information. Each principal component is a linear combination of the original variables. This PCA space was compared with other opponent color spaces by transforming various luminance and chromatic noise images into these spaces.

## 2. Experimental

### 2.1 Equipment

An IBM T221 LCD was used to display the stimuli. The 22'' LCD is 3840 by 2400 pixels, and was driven by an ATI Radeon 8500 graphic card, controlled by an Apple dual processor G5. The white point of the LCD was 250 cd/m$^2$, measured with an LMT photometer. The display was colorimetrically characterized using an LMT colorimeter using techniques described in reference 15. The average DE00 for all measurements is 1.

### 2.2 Subjects

Twenty-five observers including fourteen naive and eleven experts served as subjects. The age ranged between 23 and 43. All the subjects had normal color vision and normal or corrected-to-normal visual acuity.

### 2.3 Stimuli

Each stimulus was a chromatic noise image made of two additive complimentary colors. Stimuli were created for combinations of three relative luminance levels corresponding to $L^*$ values of 30, 50, and 70 relative to display white (Y=0.1, 0.29, 0.65), and four complementary hue pairs. One end of each pair was defined in a u'v' chromaticity space relative to the unique hues in CIELAB space (unique Yellow, unique Red, half way between Yellow and Red, half way between Red and Blue). See Figure 1 for details. The other end of the noise vector was defined as the additive complimentary going through the white-point with equal u'v' steps. Two "chroma" levels were examined. Three spatial frequency bands: an octave filter centered at 1 cpd (50% at 0.5 & 2 cpd), another centered at 4 cpd (50% at 2 & 8 cpd), and uniform white noise with a maximum frequency of 60 cpd were also used. In all this represents 72 combinations of 4 color-vectors, 2 saturations, 3 luminance levels and 3 frequency bands that were evaluated. Figure 2 shows the four color vectors for two chroma levels in u'v' space. The blue long lines represent high chroma, and red short lines represent low chroma. Each stimulus trial was repeated four times for a total of 288 settings by each observer.

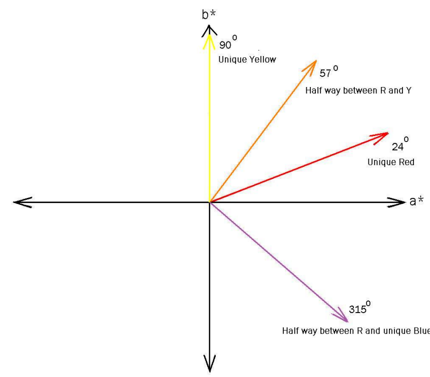


*Figure 1. Hue angles (CIELAB) used to guide selection of the complementary hue vectors. (Ref. 16)*

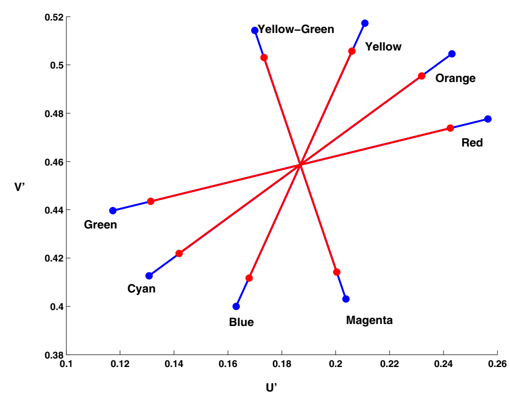


*Figure 2. Four vectors for two "chroma" levels. Blue long lines represent high chroma; red short lines represent low chroma.*

Experimental noise images were created as follows. First, a random noise image was created. This noise image was filtered using octave spatial filters to obtain the desired spatial frequency noise patterns. An octave filter is a special

Gaussian filter in log frequency space. Full Width Half Height (FWHH) occurs at half and twice the frequency of the peak. Then a color map representing a line connecting the two endpoints in the three dimensional space u'v'Y was constructed. One end of the hue pair had fixed chromaticity and luminance. The chromaticity of the other end was fixed such that it was an equal distance from the white point as the fixed end in u'v' space. The observers were asked to adjust the luminance of the other end (thus also adjusting the slope of the line connecting the endpoints) until the chromatic noise was least perceptible, e.g. the noise field was most uniform. The observers did not necessarily know that the luminance of one end was fixed. Some stimuli examples are shown in Figure 3. The first row shows all four color-vectors at one luminance and spatial frequency. The second row shows all three luminance levels for one color-vector and frequency. The third row shows all three frequency bands for one luminance and color-vector.

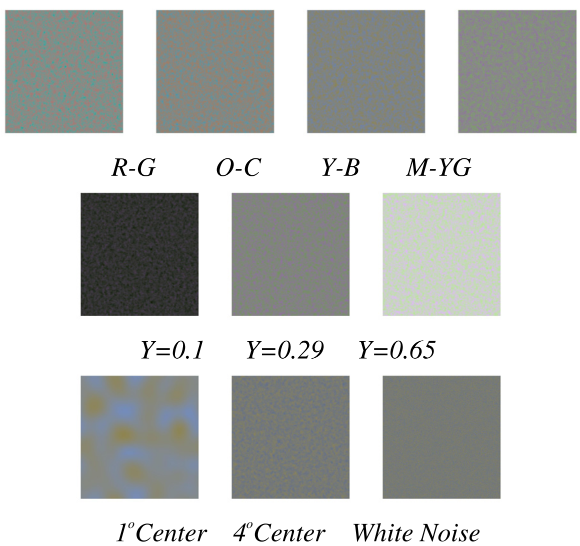


*Figure 3. Stimuli examples presented in the experiment*

## 2.4 Procedure

The stimulus was centered on the characterized IBM LCD as shown in Figure 4, with a viewing distance of three feet, subtending four degrees of visual angle. The background was set to 50% percent of Y of the white point of the display and subtended about 12° of visual angle. The remainder of the display was masked. The experiment was divided into two sessions and each session consisted of two repetitions of each of the 72 stimuli.

Most observers felt it more difficult to minimize the appearance of noise for low frequency stimuli. This is expected since the contrast sensitivity for chromatic variation is much more sensitive to low frequency information. In effect, the observers were setting the patterns to constant perceived luminance under the hypothesis that luminance noise is more easily perceived than chromatic noise.

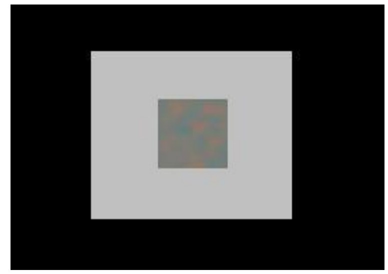

*Figure 4. Stimuli presentation in the psychophysical experiment.*

# 3. Results and Discussion

## 3.1 Inter and Intra-Observer Variance

Inter-observer and intra-observer standard deviation (STD) is reported in Figures 5 and 6. The inter-observer STD is rather small, ranging from 0.01 to 0.05 relative CIE Y units, 0-1 range. At the low luminance level, STD is smaller than that at higher luminance level. Of note, these results do not strictly follow Weber's law, with the uncertainties (a measure of thresholds) increasing more slowly than predicted by Weber's law. When subjects performed the experiment they found it more difficult for higher luminance stimuli, but much easier for lower luminance stimuli. This might be related to the overall increase in both luminance and chromatic contrast sensitivity at higher luminance levels. Intra-observer STD, as shown in Figure 6 is of a similar magnitude to the inter-observer STD.

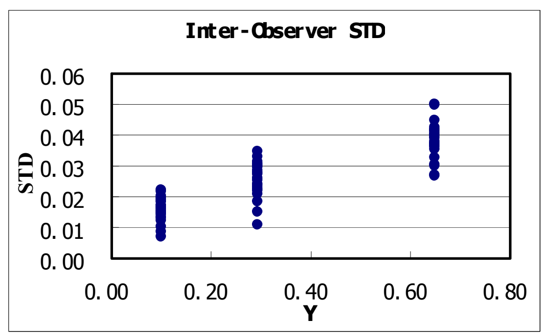


*Figure 5. Inter-observer STD.*

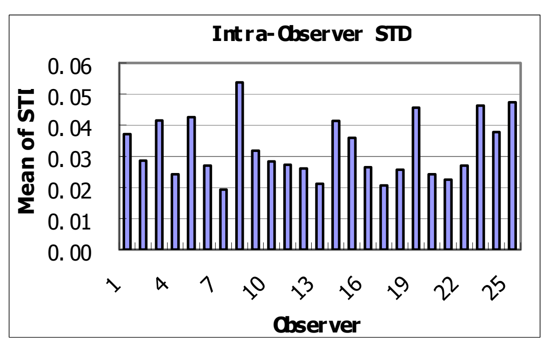


*Figure 6. Intra-observe STD.*

Of particular interest for this experiment are any possible effects of frequency, luminance and chroma on observer STD. Figure 7 illustrates that at the lowest frequency the STD is the smallest compared to the intermediate and high frequencies. According to chromatic contrast sensitivity functions, the human visual system has higher sensitivity for low frequency than for high frequency. This indicates that chromatic contrast is easier to distinguish at lower frequencies than at higher frequencies even though observers felt it more difficult for low frequency stimuli during the experiment. This might be the reason for the smaller STD at low frequencies. Figure 8 illustrates that differences in chroma appear to have no effect on STD.

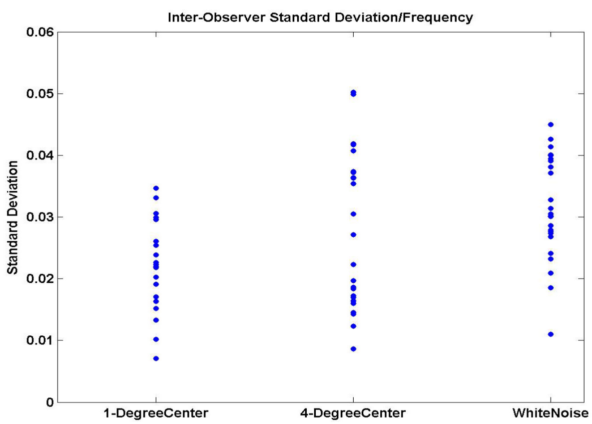


*Figure 7. Variance was calculated among all observers and classified according to spatial frequency.*

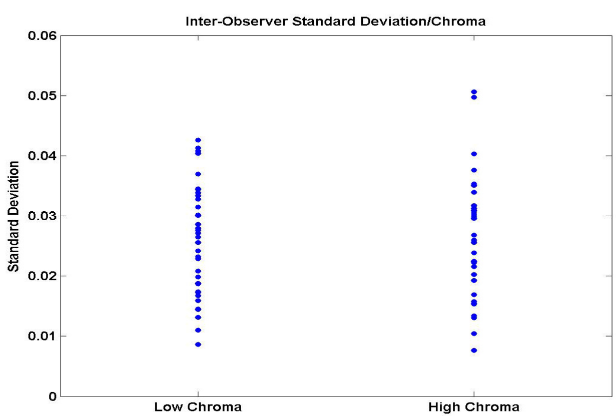


*Figure 8. Variance was averaged among all observers and classified according to chroma*

### 3.2 Principle Components Analysis

To address the question of finding the color space that best separates luminance and chrominance information, the data distribution in three dimensions (such as CIE XYZ) must be examined. Figures 9a and 9b illustrate that all data vary more along the X and Z dimensions, but much less along the Y dimension. From the figures one can see that most of the data variation is orthogonal, or nearly orthogonal to Y. This immediately suggests that the CIE 1931 Y dimension is a reasonable predictor of *perceived* luminance for this application.

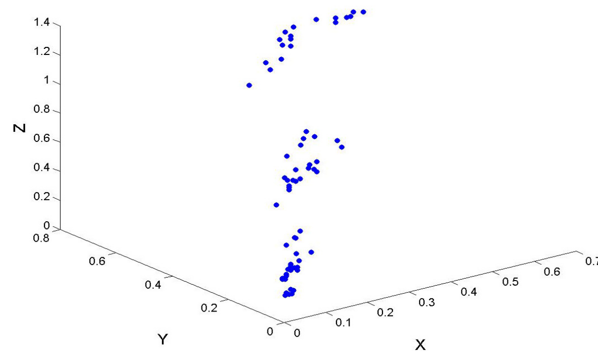


*Figure 9a. Data in XYZ space. Data shown here are final XYZ of the adjustment end averaged among all observers and four repetitions.*

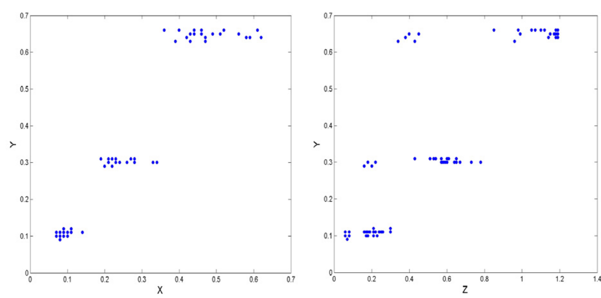


*Figure 9b. Data projected onto X-Y (left) and Z-Y (right) plane.*

Figure 10 shows the data visualized in another way with each line drawn between the fixed end (left) and the observer adjustment end (right). Each row has the same luminance. Each column has the same color-vectors but with two levels of chroma. The short line represents low chroma pairs and the long line represents high chroma pairs. For each subplot there are six combinations of two chroma levels and three frequencies. It is assumed that when the *perceived* luminance of the two ends (and every point between) is equal, the chromatic noise will be least perceptible. As expected, the CIE luminance of the two ends is similar. It is interesting to note that for higher luminance (bottom row Figure 10), the scatter is larger than that for lower luminance.

The standard deviation ranges among all observers for each subplot are shown in Table 1. Table 1 illustrates that for high luminance levels, the variance is larger, while for low luminance levels, the variance is smaller. In all cases, the CIE Y differences between the end-points are of the same order as, or smaller than the standard deviation between observers.

A statistical T-test was applied to determine if there were significant difference between CIE Y value of the adjusted endpoint and the Y value of the anchor point. From the test 41 out of the 72 stimuli showed a significant difference between the CIE Y of the two end-points.

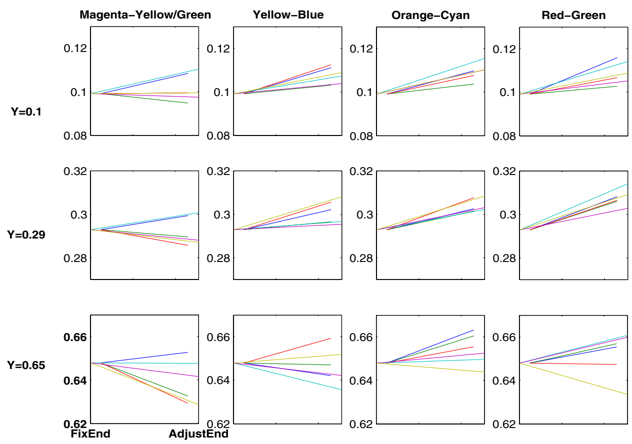


*Figure 10. The x-axis of each subplot indicates fixed end and adjustment end as shown on the left corner plot. The blue and cyan lines represent stimuli with frequency centered at 1 cpd, the green and magenta line centered at 4 cpd, and the red, yellow line for white noise. Short or long lines are used to distinguish low or high chroma respectively.*

**Table 1. Variance Range for Each Subplot in Figure 12**

| Luminance Level | | M-Y/G | Y-B | O-C | R-G |
|---|---|---|---|---|---|
| Y=0.1 | Min | 0.01 | 0.01 | 0.01 | 0.02 |
| | Max | 0.02 | 0.02 | 0.02 | 0.02 |
| Y=0.29 | Min | 0.01 | 0.02 | 0.02 | 0.03 |
| | Max | 0.03 | 0.03 | 0.03 | 0.03 |
| Y=0.65 | Min | 0.03 | 0.03 | 0.04 | 0.04 |
| | Max | 0.04 | 0.04 | 0.04 | 0.05 |

Principle Components Analysis was applied on the data at each initial lightness values. The function pcacov.m in Matlab[17] was used to perform PCA. The input to the PCA is the CIE XYZ values of the two endpoints for each luminance level. Equations 1.1, 1.2, 1.3 show the calculated transformations from XYZ into the three dimensions of the PCA space (for each initial luminance level). From the PCA we can see that the third dimension contributes near zero variance (see Table 2). Notice from Equations 1.1-1.3 that this dimension correlates very strongly with the CIE Y luminance channel. In Table 2, the small percentage value for the third dimension indicates that the input data varies much less in that dimension than the first two dimensions. The principle component matrices constitute a preliminary orthogonal color space, and give a good starting point for the creation of a new opponent color space specifically designed for image processing. The PCA space also allows for summary of the data to evaluate historical color spaces.

For Y=0.1

$$\begin{bmatrix} V_1 \\ V_2 \\ V_3 \end{bmatrix} = \begin{bmatrix} -0.0249 & -0.0480 & -0.9985 \\ 0.9936 & -0.1114 & -0.0194 \\ -0.1103 & -0.9926 & 0.0505 \end{bmatrix} * \begin{bmatrix} X \\ Y \\ Z \end{bmatrix} \tag{1.1}$$

For Y=0.29

$$\begin{bmatrix} V_1 \\ V_2 \\ V_3 \end{bmatrix} = \begin{bmatrix} -0.0048 & 0.0196 & 0.9998 \\ -0.9983 & 0.0578 & -0.0059 \\ -0.0579 & -0.9981 & 0.0193 \end{bmatrix} * \begin{bmatrix} X \\ Y \\ Z \end{bmatrix} \tag{1.2}$$

For Y=0.65

$$\begin{bmatrix} V_1 \\ V_2 \\ V_3 \end{bmatrix} = \begin{bmatrix} -0.0279 & 0.0064 & 0.9996 \\ -0.9996 & -0.0018 & -0.0279 \\ 0.0016 & -1.0000 & 0.0064 \end{bmatrix} * \begin{bmatrix} X \\ Y \\ Z \end{bmatrix} \tag{1.3}$$

**Table 2. Variance and Percent Variance Explained by Each Dimension from PCA**

| Luminance Level | V1 | V2 | V3 |
|---|---|---|---|
| Y=0.1 | 0.0059 (95.51%) | 0.0003 (4.26%) | 0 (0.23%) |
| Y=0.29 | 0.0425 (94.53%) | 0.0024 (5.42%) | 0 (0.05%) |
| Y=0.65 | 0.1267 (92.75%) | 0.0099 (7.21%) | 0 (0.04%) |

### 3.3 Chromatic Noise Prediction

As illustrative examples shown, the visibility of chromatic noise in the PCA space and other color spaces can be visualized.

Various noise images used in the experiment with combinations of different frequency, luminance and chroma were transformed to CIE XYZ, and then to the PCA space and other opponent spaces. The PCA space defines optimal performance for this data-set, and other opponent color spaces can be compared to look for similar capabilities. Figure 11 gives examples of a noise image along the yellow-blue vector expressed in individual channels of the PCA space, CIE XYZ, IPT, YCbCr and YIQ. Linear in luminance versions of each space were used.

For this noise image, in the PCA (the first row) space, noise is barely present in the third dimension, and little noise is observed in the Y channel of CIE XYZ, YCbCr and YIQ spaces, while in the IPT space there is some noise apparent in the achromatic channel. This implies that IPT color space is not orthogonal with luminance and might be sub-optimal for chromatic noise evaluation, modeling and perceptibility prediction. The fact that noise varies in chromatic channels for different spaces indicates the color direction of the chromatic channels. For example, for this yellow-blue noise image, in IPT space there is less noise observed in the P channel than that in the T channel, because the P channel is along red-green direction, and the T channel is along yellow-blue direction, suggesting the most noise in this channel for this yellow-blue noise image.

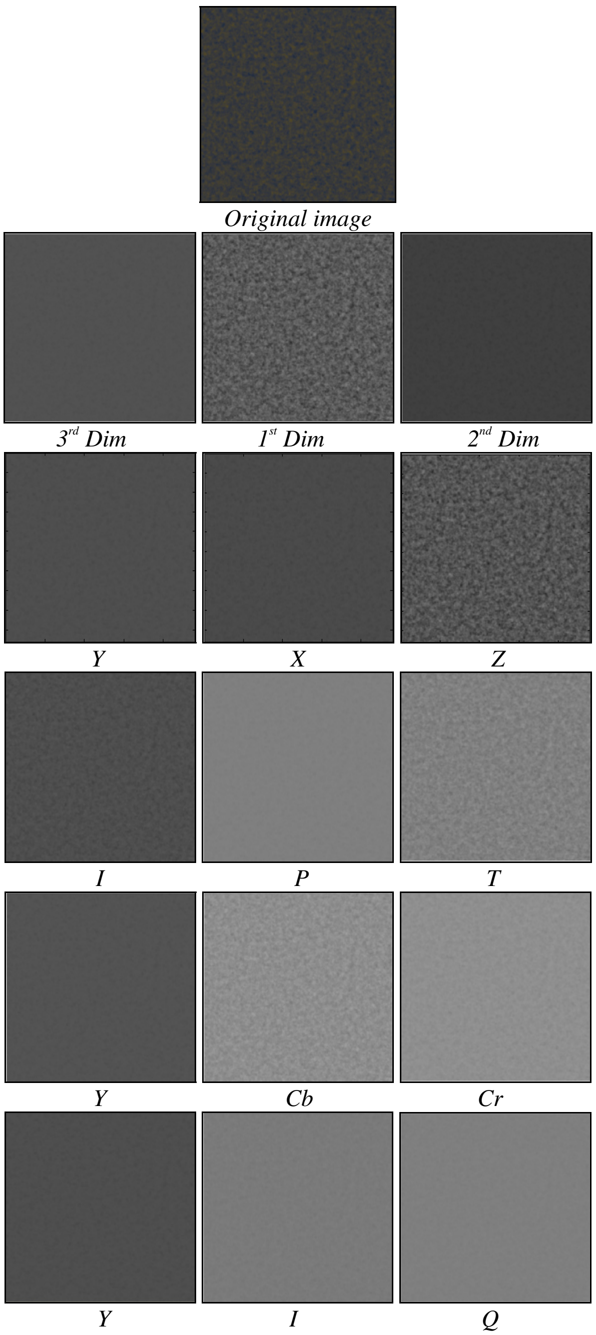


*Figure 11. The top is the original image. Stimulus information is u'v' of 0.2108 and 0.5173 respectively, luminance level 0.1, and 4cpd spatial frequency. The rest are the same image transformed into various color spaces.*

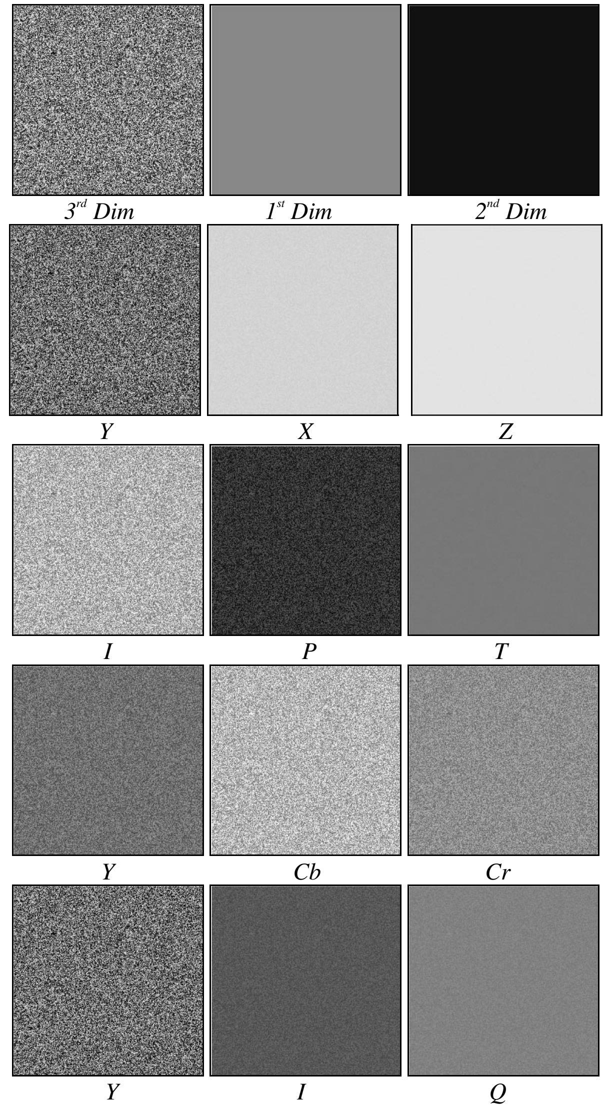


*Figure 12. Cross-talk of luminance noise into chromatic channels in various color spaces.*

Figure 12 illustrates cross-talk of luminance noise into chromatic channels in various color spaces. These images were created by making a neutral gray in sRGB and then converting that image into XYZ and then the PCA space. Noise was added to the third dimension of the PCA space and then converted back into XYZ. From there the image was converted to the various color spaces. Most noise is permuted to the luminance channel for all the spaces. There is noise "leakage" into the P channel of the IPT space, and all the channels of the YCbCr space, while slightly less into the I and Q channel of YIQ, and the T of IPT. This illustrates how the PCA space was optimized to serve as an orthogonal color space for chromatic noise prediction and modeling. Figure 12 also illustrates the limitations of using some of the other color spaces for predicting the visibility of chromatic noise since luminance noise leaks into the chromatic dimensions and vice versa.

## 4. Conclusion

A psychophysical experiment was performed to measure the visibility of chromatic noise. Observers minimized the visibility of noise patterns of various spatial frequencies, luminance levels, and hues. An orthogonal color space has been derived to describe these data using Principal Component Analysis. This space was used to examine historical opponent spaces by transforming various chromatic noise images into this PCA space and other opponent color spaces. The cross-talk of luminance noise into chromatic channels was also examined. These results will be used to optimize models of chromatic noise perception for digital imaging. More experiments are to be performed to measure the threshold and suprathreshold noise perception in the PCA color space. Comparisons will also be made with additional opponent color spaces. It is hoped that an optimal opponent color space for use in image quality metrics, image difference metrics, image compression, and other digital image processing can be created for use with an optimized set of CSFs.

## 5. References


1. Rafael C. Gonzalez and Richard E. Woods, Digital Imaging Processing, 2nd edition, 2002. *Prentice Hall.*
2. M.D. Fairchild and G.M. Johnson, The iCAM framework for image appearance, image differences, and image quality. *Journal of Electronic Imaging,* (2004).
3. Xuemei Zhang, and Brian A. Wandell, A spatial extension of CIELAB for digital color image reproduction, *Proceedings of the SID Symposium*, 731-734 (1996).
4. B. A. Wandell, Foundation of Vision (1995), *Sinauer Press, Sunderland MA.*
5. G. Guchsbaum and A. Gottschalk, Trichromacy, opponent colours coding and optimum colour information transmission in the retina, *Proc. R. Soc. Lond. B* 220, 89-113 (1983).
6. B. Poirson and B. A. Wandell, Appearance of colored patterns: pattern-color separability, *Journal of the Optical Society of America*, 10(12), 2458-2470.
7. B. Poison & B. A, Wandell (1996), Pattern-color separable pathways predict sensitivity to simple colored patterns. *Vision Research*, Vol. 36, No. 4, 515-526.
8. S. L. Guth, The chromatic contrast sensitivity myth, *The 5th Color Imaging Conference: Color vision*, 23-26.
9. H. C. Owens, et al, Contrast Sensitivity for lime-purple and cyan-orange gratings, *IS&T/SID Tenth Color Imaging Conference*, 145-148.
10. Charles A. Poynton, A technical introduction to digital video (1996), *John Wiley & Sons, Inc.*.
11. M. W. Schwarz, et al, An experimental comparison of RGB, YIQ, LAB, HSV, and opponent color models, *ACM Transactions on Graphics*, Vol. 6, No. 2, April 187, 123-158.
12. F. Ebner & M. D. Fairchild, Development and testing of a color space (IPT) with improved hue uniformity, *IS&T/SID 6th Color Imaging Conference*, 8-13.
13. S. Y. Zhu et al, New uniform color spaces, *IS&T/SID 10th Color Imaging Conference*, 61-65.
14. Silvio Borer and Sabine Süsstrunk, Opponent color space motivated by retinal processing. *CGIV 2002: The first European conference on color graphics, imaging and vision*, 187-189.
15. Elen Day, et al, Colorimetric characterization of a computer-controlled Liquid Crystal Display, *Color Research Application*, in press (2004).
16. Mark D. Fairchild, Color appearance models, *Addison Wesley*, 1998
17. MATLAB: The language of Technical Computing, Version 6.5 Release 6, 2002. *Mathworks, Inc*.


## Biography

**Xiaoyan Song** received her B.S. degree in Information Management and Information System from Shandong University at China in 2000. She will receive her M.S degree in Color Science from Rochester Institute of Technology in 2004. Her thesis research is on chromatic noise perception in digital photography. Other research interests are on color management, image appearance modeling and psycho-physics experiment design.